PCCP

A Comparison Between Hydrogen and Halogen Bonding: The Hypohalous Acid-Water Dimers, HOX–H_2O (X=F, Cl, Br)

Journal:	*Physical Chemistry Chemical Physics*
Manuscript ID	CP-ART-01-2019-000422.R1
Article Type:	Paper
Date Submitted by the Author:	18-Feb-2019
Complete List of Authors:	Wolf, Mark; University of Georgia , Center for Computational Quantum Chemsitry Zhang, Boyi; University of Georgia , Center for Computational Chemistry Turney, Justin; University of Georgia, Center for Computational Chemistry Schaefer, Henry; University of Georgia, Computational Chemistry

Journal Name

ARTICLE TYPE

Cite this: DOI: 10.1039/xxxxxxxxxx

A Comparison Between Hydrogen and Halogen Bonding: The Hypohalous Acid-Water Dimers, HOX···H_2O (X=F, Cl, Br)†

Mark E. Wolf, Boyi Zhang, Justin M. Turney, and Henry F. Schaefer III*

Received Date
Accepted Date

DOI: 10.1039/xxxxxxxxxx

www.rsc.org/journalname

Hypohalous acids (HOX) are a class of molecules that play a key role in the atmospheric seasonal depletion of ozone and have the ability to form both hydrogen and halogen bonds. The interactions between the HOX monomers (X=F, Cl, Br) and water have been studied at the CCSD(T)/aug-cc-pVTZ level of theory with the spin free X2C-1e method to account for scalar relativistic effects. Focal point analysis was used to determine CCSDT(Q)/CBS dissociation energies. The *anti* Hydrogen bonded dimers were found with interaction energies of –5.62 kcal mol^{-1}, –5.56 kcal mol^{-1}, and –4.97 kcal mol^{-1} for X=F, Cl, and Br, respectively. The weaker halogen bonded dimers were found to have interaction energies of –1.71 kcal mol^{-1} and –3.03 kcal mol^{-1} for X=Cl and Br, respectively. Natural bond orbital analysis and symmetry adapted perturbation theory were used to discern the nature of the halogen and hydrogen bonds and trends due to halogen substitution. The halogen bonds were determined to be weaker than the analogous hydrogen bonds in all cases but close enough in energy to be relevant, significantly more so with increasing halogen size.

Introduction

In recent years, there has been increasing interest in hypohalous acids (HOX, X= F, Cl, Br) due to the critical roles they play in the seasonal depletion of ozone in the atmosphere.[1–9] Hypohalous acids are thought to be "sinks" for halogen radical species, which also directly react with ozone molecules.[10,11] Kinetics simulations have indicated that the reaction between HOCl and HCl is necessary to maintain a usable level of activated chlorine, which is a primary destroyer of ozone.[12] HOX molecules also play a prominent role in biochemistry. Their oxidative nature makes them extremely reactive with biological structures (e.g., NADH,[13] DNA,[14] heme groups,[15] cytochrome c[16]) and often leads to toxic effects in the human body. The biological toxicity of HOCl can conversely be beneficial to the human body by acting as an antibiotic for external wound care.[17] Additionally, hypohalous acids are relevant in many other fields such as molecular biology[18] and immunology.[19]

A unique trait of HOX molecules is their ability to form both hydrogen (HB) and halogen (XB) bonds. The importance of these two noncovalent interactions cannot be overstated, as they are critical to biological systems,[20] organometallic chemistry,[21] crystal structures,[22] and many other applications.[23–25] Moreover, protonated HOCl is a potential transition state for one of the key reactions leading to ozone depletion,[26] the reactivity of which can be intimately affected by existing noncovalent interactions with other atmospheric molecules. Even more pertinent to our present research is that HOX molecules are often in complex with one or more water molecules before reacting in the atmosphere.[27–29] The fact that HOX molecules can participate in both types of bonds provides a prime opportunity to study the competitive and cooperative nature of these interactions. Both Hydrogen[30–33] and halogen[34–50] bonding have been well studied experimentally and theoretically and we direct the reader to a plethora of literature on both. XB and HB are fundamentally electrostatic processes, however, the importance of dispersion forces are important to correctly model XB.[36,45,51] It is widely accepted than the hydrogen bond is the stronger of the two interactions, however, experimental and theoretical suggest that halogen bonds can be made stronger than hydrogen bonds in a variety of chemical settings.[52–56] Therefore it is beneficial to know the accurate relative strengths of the halogen and hydrogen bonds between HOX and water molecules, as it could affect atmospheric models.

Hypohalous acids are highly reactive and therefore notoriously unstable and difficult to study experimentally.[16] While spectroscopy has confirmed the presence of HOX species in the atmosphere,[57–60] only HOF has been isolated in pure crystalline form.[61] To the best of our knowledge no experimental data is available quantifying the interaction energy of the HOX molecule and water. A theoretical approach is thus quite appropriate. Pre-

* *Center for Computational Quantum Chemistry, University of Georgia, 140 Cedar Street, Athens, Georgia 30602 United States of America. Fax: (706) 542-0406; Tel: (706) 542-2067; E-mail: ccq@uga.edu*

† Electronic Supplementary Information (ESI) available: [details of any supplementary information available should be included here]. See DOI: 10.1039/b000000x/

vious research groups have published computational studies on the intermolecular interactions between HOX species and other molecules.[52,62–71] By far the most common theory employed in the treatment of these complexes is second order Møller–Plessest (MP2) theory, often complemented with density functional theory (DFT). A non-exhaustive list of recent publications includes HOX structural formations with formaldehyde, formamidine,[62] formyl halides,[64] phosphorus ylide,[72]ozone,[66] and sulfoximine.[67] The motivation for most of these studies is to analyze the nature of the hydrogen and halogen bonds that are formed and how the bonding nature changes across the halogen series. In particular, the halogen bond has quite variable strength depending on the halogen atom involved.[37,52] Properly explaining this trend is key to a foundational understanding of the relative strength of these noncovalent interactions in more complex chemical settings. The most comprehensive theoretical study to date of the HOX and water dimer is that of Panek and Berski that used DFT to study the hetero and homo dimers of HOX (X= F, Cl, Br) with water.[73] They determined that DFT increasingly underestimated the interaction energies with a B3LYP functional compared to MP2 (with the same basis set) as the size of the halogen increased. They also applied symmetry adapted perturbation theory (SAPT) to decompose the interaction energy of the noncovalent interactions into physically meaningful components, which varied significantly depending on the halogen involved. Their SAPT results predicted that dispersion interactions were of critical importance to XBs but not HBs agreeing with the research Anderson and coworkers on halogen bonding in general.[36] A similar paper by Zhang and coworkers used MP2/aug-cc-pVTZ to study all of the homodimers of HOCl.[74] They found six structures and determined with natural bond orbital analysis (NBO) that, for most structures, donor-acceptor and charge transfer interactions contributed primarily to complex formation. The NBO analysis also confirmed that dispersion interactions were less important relative to electrostatic forces in five out of six structures, in disagreement with the findings of Panek and Berski.[73] Multiple theoretical studies have also been published that specifically study dimers formed between HOX and water. An early DFT study of the $HOBr\cdots H_2O$ was performed by Ying and Zhao in 1997.[75] Santos and coworkers mapped the MP2 potential energy surface of $HOBr\cdots H_2O$ in 2004,[76] and provides the most accurate structures to date optimized at the CCSD/6-311++G(2d,2p) level of theory. They determined that electron correlation had little effect on interaction energies. In 1995, Dibble and Franciso presented MP2/6-311++G(d,p) geometries along with interaction energies for HOCl and water dimers.[27] Qiao and coworkers have published related MP2 work on $HOBr\cdots H_2O$ dimers.[77]

Despite the variety of HOX compounds studied in the literature, there is insufficient theoretical rigor in the previously mentioned publications. Most studies use modest (by 2019 standards) levels of theory to optimize geometries and compute energetics. Although DFT functionals may capture interaction energies, there exists no high level *ab initio* study to confirm these results. Thus, we cannot know *a priori* if the functionals used are appropriate. Similarly, many studies use basis sets that may be insufficient. For example, a paper by Zhang and coworkers presents structures for HOCl dimers using the aug-cc-pVTZ basis set.[74] However, Dunning and coworkers have published research that establishes the importance of additive tight *d* functions in obtaining accurate descriptions of molecules containing Al-Ar atoms.[78] Likewise, none of the previous studies comment on relativistic effects that may arise from heavier atoms like Cl and Br. Failing to account for relativity in heavier atoms can seriously skew the true periodic trends of halogen bonding. The combination of these sources of error creates a need for more rigorous study of these systems. Our work seeks to provide a rigorous and accurate theoretical study of the dimers formed by HOX molecules and water. Accurate HOX/water structures are computed at the CCSD(T) level of theory, along with a focal point approach to obtain CCSDT(Q)/CBS interaction energies. Proper treatment of scalar relativistic effects is included. An in depth analysis into the nature of HB and XB interactions is provided. Our results can be used as a theoretical benchmark for any future studies pertaining to HOX species.

Methods

Equilibrium geometries were optimized for the HOX monomers (X=F,Cl,Br), H_2O, $HOX\cdots OH_2$, and $XOH\cdots OH_2$ structures using coupled cluster theory with single, double, and perturbative triples excitations [CCSD(T)][79–82] as implemented in the software package CFOUR.[83,84] Harmonic vibrational frequencies were computed to ensure each structure was a minimum on its potential energy surface. The SCF density, coupled cluster amplitudes, and lambda equations were converged to 10^{-10}. Since we are studying heavy atoms, the inclusion of relativistic effects are needed. The standard one-electron Hamiltonian was augmented with the one-electron variant of the spin-free exact two-component Hamiltonian (SFX2C-1e)[85–87] to include scalar relativistic effects for both geometry optimization and harmonic vibrational frequency computations. The use of the SFX2C-1e method requires properly contracted relativistic basis sets. Since the Dunning basis sets are nonrelativistic basis sets, we used the X2C recontracted basis sets available on the CFOUR website.[88] The X2C-aug-cc-pVTZ basis set[89] was used for all bromine and fluorine structures, and the X2C-aug-cc-pV(T+d)Z basis set[78] was used for all chlorine atoms.[36] All computations were performed with the frozen core approximation. Preliminary tests agreed with previous research claiming that for a proper description of heavy atom halogen bonds, the 3*d* electrons needed to be correlated for all bromine containing structures.[90,91] Therefore, the X2C-aug-cc-pCVXZ basis[92] set was employed for all structures including bromine atoms.

Interaction energies, $E_{int} = E_{dimer} - (E_{HOX} + E_{H_2O})$, were determined by means of the focal point method developed by Allen and coworkers.[93–96] The three point formula of Feller[97] was used to extrapolate HF energies while the two-point formula of Helgaker[98] was used to extrapolate each post-HF energy. Each extrapolated component is then summed to obtain a CCSDT(Q)/CBS interaction energy. The SFX2C-1e one-electron Hamiltonian was used for our extrapolated energies, along with the X2C recontracted Dunning basis sets. The focal point computations were performed on the CCSD(T)/X2C-aug-cc-pVTZ optimized geometries. The CCSDT(Q)/CBS energies were then cor-

rected to account for approximations used in previous computations. The zero-point vibrational energy correction, ΔE_{ZPVE}, was computed at the CCSD(T)/X2C-aug-cc-pVTZ level of theory. The diagonal Born–Oppenheimer correction, ΔE_{DBOC}, were computed at the Hartree–Fock level of theory with the same basis set to account for the assumption of fixed nuclei.[99,100] A frozen core correction, $\Delta E_{FC} = E_{AE} - E_{FC}$, was also computed to account for core electron correlation. E_{AE} and E_{FC} were computed at the CCSD(T)/X2C-aug-cc-pCVTZ level of theory with all electrons and only the valence electrons correlated, respectively.[101] For bromine atoms, the 3*d* electrons were not included in the frozen core approximation. Thus, the final focal point energy for each structure is given by, $E_{final} = E_{CCSDT(Q)-X2C/CBS} + \Delta E_{ZPVE} + \Delta E_{FC} + \Delta E_{DBOC}$. The corrected energies are used to obtain the interaction energies between HOX monomer and water.

Natural bond order (NBO) analysis was performed to assess the donor and acceptor nature of the bonding orbitals.[102] The NBO6.0 package[103] as interfaced to QCHEM[104] was used to compute the second-order perturbation energy, $E^{(2)}$ of a hybrid orbital overlap (Equation 1).

$$E^{(2)} = q_i \frac{F_{ij}^2}{\varepsilon_j - \varepsilon_i} \quad (1)$$

F_{ij} is defined as the NBO Fock matrix element between donor natural bond orbital i and acceptor natural bond orbital j. ε_i and q_i are defined as the orbital energy and orbital occupation, respectively, of natural bond orbital i. The B3LYP functional[105] with the aug-cc-pVDZ basis set was used for all NBO computations. The orbitals were visualized using the software package Jmol.[106]

Symmetry adapted perturbation theory (SAPT) was used to dissect the interaction energies of the hydrogen and halogen bonds into physically meaningful components: dispersion, induction, exchange, and electrostatic (Equation 2).[107,108] A more detailed description of the decomposition scheme is available in the supplementary information. SAPT2+3 computations were performed using the PSI4[109] software package with the standard aug-cc-pVTZ basis.

$$E_{SAPT2+3} = E_{Electrostatic} + E_{Exchange} + E_{Induction} + E_{Dispersion} \quad (2)$$

Results and Discussion

Equilibrium Geometries

Two types of favorable interactions were found between the HOX monomer and water. One was a dimer formed by a hydrogen bond between the hydrogen on the hypohalous acid and the oxygen in water. These hydrogen bonded (HB) dimers are denoted as XOH$\cdots$OH$_2$. The second type of interaction was a halogen bond formed between the halogen of the HOX monomer and the oxygen of water. These halogen bonded (XB) dimers are denoted as: HOX$\cdots$OH$_2$. For the XOH$\cdots$OH$_2$ dimers, geometries were found for X=F and Cl with each having both a *syn* and *anti* conformer (Figure 1). For X=Br, the *anti* conformer was a minimum on the potential energy surface, but the C_S *syn* conformer was not (22*i* cm^{-1} vibrational mode). Panek and Berski found this minimum

Fig. 1 CCSD(T)/aug-cc-pVTZ-X2C optimized geometries for the hydrogen bonded dimers. The *syn* conformers are shown on the left and the *anti* conformers on the right. The hydrogen bond lengths (in Å) and internal X-O-H angles (in degrees) are shown. Atoms are colored gold, green, and purple for F, Cl, and Br, respectively.

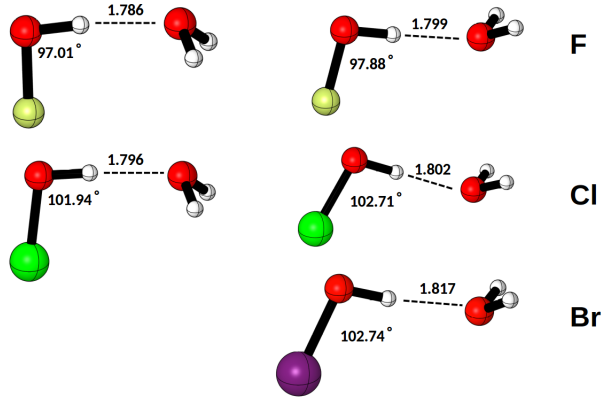

Fig. 2 CCSD(T)/aug-cc-pVTZ-X2C optimized geometries for the halogen bonded dimers. The *syn* conformers are shown on the left and the *anti* conformers on the right. The halogen bond lengths (in Å) and internal H-O-X angles (in degrees) are shown. Atoms are colored green and purple for Cl and Br, respectively.

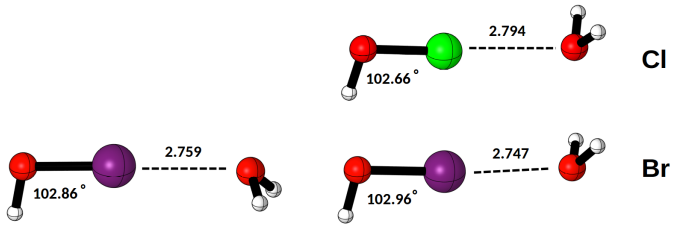

syn structure at the MP2/aug-cc-pVTZ level of theory to have a dihderal of 3.2°.[73] Scans were performed to search for a structure that was not C_S but the potential energy surface was found to be too shallow for a minimum structure at our level of theory. The *syn* dimers were slightly more favorable energetically by 0.07 and 0.11 kcal mol^{-1} for X=F and Cl, respectively.

For the halogen bonded dimers, geometries were found for X = Cl and Br. Both *syn* and *anti* conformers were found for HOBr$\cdots$OH$_2$, but only the *anti*-HOCl$\cdots$OH$_2$ structure was found for chlorine (Figure 2). The *anti*-HOBr–OH$_2$ conformer is the more favorable conformer by 0.14 kcal mol^{-1}. A structure for *syn*-HOCl–OH$_2$ was optimized but was not a minimum on the potential energy surface (35*i* cm^{-1} vibrational mode). This imaginary mode was due to the torsional vibration about the halogen bond. We agree with previous theoretical research that was unable to find any HOF$\cdots$OH$_2$ structure. This in part due to the fact that fluorine is more electronegative than oxygen and thus HOF does not have a significant sigma hole on F.

Optimized geometries were computed for all HOX monomers and water so that accurate interaction energies could be computed. All structures presented have C_S symmetry. We also considered interactions between a hydrogen from water and the oxygen of HOX, but no such structures were found. All geometri-

cal structures reported here were confirmed to be minima on the potential energy surface by computing harmonic vibrational frequencies. Cartesian coordinates for all structures are provided in the supplementary information.

The most important geometric parameters for each dimer are presented in (Figure 1). We highlight the distance between the hydrogen atom of the HOX and water as well as the internal bond angle of the HOX atoms within the dimer structure. These parameters are perhaps the most relevant and interesting with respect to understanding the nature of halogen or hydrogen bonding in these species. For the *syn*-XOH$\cdots$OH$_2$ structures, the hydrogen bond lengths (1.786 Å, 1.796 Åfor F ,Cl), increase slightly going down the halogen series. The *anti*-XOH$\cdots$OH$_2$ structures follow a similar trend (1.799 Å, 1.802 Å, 1.817 Å for F, Cl, Br) Panek and Berski computed MP2 structures with larger hydrogen bond distances of 1.806 Å, 1.808 Å, 1.822 Å,[73] respectively. Santos and coworkers, who optimized geometries with CCSD/6-311++G(2d,2p), also overestimated the *syn*-BrOH$\cdots$OH$_2$ hydrogen bond at 1.858 Å.[76] This especially large difference may be explained by our inclusion of the perturbative triples correction, as well as the use of the X2C method to obtain a scalar relativistic corrected geometry. The effect of halogen substitution on the geometries decreases with increasing halogen size. This is most simply due the decrease in the electronegativity of the halogen atom, which lowers the ability of the hydrogen to accept electron density from water. The internal HOX bond angles follow a much less linear trend. For the *anti* isomers, the fluorine dimer has an angle of 97.88° and the chlorine and bromine dimers have angles 102.71° and 102.74°, respectively. The *syn* isomers follow a similar trend but are approximately 1° smaller than the *anti* isomers.

The HOX$\cdots$OH$_2$ dimers have very different geometric parameters compared to the XOH$\cdots$OH$_2$ dimers. The energetically favorable *ani* isomers have halogen bond distances of 2.794 Å for the chlorine structure and 2.747 Å for the bromine structure. This is a reversal of the trend for the HB dimers down the halogen series. An explanation is that the larger and more diffuse halogens can be induced to form a positive σ hole that accepts electron density from water.[110] We can only compare the *anti* dimers to the one *syn*-HOBr$\cdots$OH$_2$ structure found, but we note a slight elongation of the XB to 2.759 in the *syn* isomer. The internal HOX bond angle increases from 102.7° in the chlorine dimer to 103.0° in the bromine dimer. There is a slight decrease in the HOX angle from the bromine *anti* to the *syn* isomer.

Interaction Energies

The focal-pointed CCSDT(Q)/CBS interaction energies with additive corrections for the XOH$\cdots$OH$_2$ dimers are presented in Table 1. The additive ZPVE correction was approximately 1 kcal mol^{-1} for XB dimers and 2 kcal mol^{-1} for HB dimers. The DBOC and frozen core corrections were much smaller, on the order of 0.01 kcal mol^{-1} for the XOH$\cdots$OH$_2$ structures. The interaction energies for the *syn* isomers were –5.62 kcal mol^{-1} and –5.56 kcal mol^{-1} for X=F and Cl, respectively. The *anti* structures had slightly smaller magnitude interaction energies of –5.37 kcal mol^{-1}, –5.28 kcal mol^{-1}, and –4.97 kcal mol^{-1}, respectively. Therefore the substitution of different halogen atoms has little effect on the strength of the hydrogen bonds. This is consistent with the trend seen in the bond lengths. The significance of the CCSDT correction increased as the size of the halogen increased from 0.01 kcal mol^{-1} for fluorine to 0.03 kcal mol^{-1} for bromine. The CCSDT(Q) correction is minimal for all structures indicating convergence with respect to level of theory.

Table 1 Focal-point analysis of the interaction energies of the hydrogen bonded XOH$\cdots$OH$_2$ structures in kcal mol^{-1}. The CCSD(T)/X2C-aug-cc-pVTZ equilibrium geometries were used for all computations here. Bracketed values indicate extrapolated energies or corrections. δ indicates an incremental change in the energy from the previous level of theory. The CCSDT(Q)/X2C-CBS interaction energies and corrections are shown below in accordance to the formula: $E_{final} = E_{CCSDT(Q)-X2C/CBS} + \Delta E_{ZPVE} + \Delta E_{FC} + \Delta E_{DBOC}$

syn-FOH$\cdots$OH$_2$

	HF	+δ MP2	+δ CCSD	+δ (T)	+δ T	+δ (Q)	NET
aug-cc-pVDZ	–6.76	–1.52	+0.28	–0.46	+0.01	+0.00	–8.44
aug-cc-pVTZ	–6.39	–1.69	+0.25	–0.43	+0.01	[+0.00]	[–8.25]
aug-cc-pVQZ	–6.28	–1.68	+0.29	–0.43	[+0.01]	[+0.00]	[–8.08]
aug-cc-pV5Z	–6.22	–1.64	+0.31	–0.42	[+0.01]	[+0.00]	[–7.96]
CBS LIMIT	[–6.18]	[–1.60]	[+0.32]	[–0.42]	[+0.01]	[+0.00]	[–7.87]

E$_{int}$ = –7.87+2.17+0.06+0.02 = **–5.62**

anti-FOH$\cdots$OH$_2$

	HF	+δ MP2	+δ CCSD	+δ (T)	+δ T	+δ (Q)	NET
aug-cc-pVDZ	–6.53	–1.29	+0.28	–0.37	+0.01	+0.00	–7.89
aug-cc-pVTZ	–6.24	–1.41	+0.25	–0.33	+0.01	[+0.00]	[–7.72]
aug-cc-pVQZ	–6.16	–1.40	+0.29	–0.33	[+0.01]	[+0.00]	[–7.59]
aug-cc-pV5Z	–6.11	–1.36	+0.30	–0.32	[+0.01]	[+0.00]	[–7.48]
CBS LIMIT	[–6.07]	[–1.31]	[+0.31]	[–0.32]	[+0.01]	[+0.00]	[–7.39]

E$_{int}$ =–7.39+1.94+0.06+0.02 = **–5.37**

syn-ClOH$\cdots$OH$_2$

	HF	+δ MP2	+δ CCSD	+δ (T)	+δ T	+δ (Q)	NET
aug-cc-pV(D+d)Z	–5.79	–2.27	+0.53	–0.48	+0.03	–0.01	–7.99
aug-cc-pV(T+d)Z	–5.52	–2.54	+0.54	–0.49	+0.03	[–0.01]	[–8.00]
aug-cc-pV(Q+d)Z	–5.43	–2.53	+0.57	–0.49	[+0.03]	[–0.01]	[–7.87]
aug-cc-pV(5+d)Z	–5.39	–2.51	+0.58	–0.49	[+0.03]	[–0.01]	[–7.8]
CBS LIMIT	[–5.46]	[–2.49]	[+0.60]	[–0.49]	[+0.03]	[–0.01]	[–7.74]

E$_{int}$ = –7.74+2.09+0.07+0.02 = **–5.56**

anti-ClOH$\cdots$OH$_2$

	HF	+δ MP2	+δ CCSD	+δ (T)	+δ T	+δ (Q)	NET
aug-cc-pV(D+d)Z	–5.73	–1.98	+0.48	–0.41	+0.03	–0.01	–7.63
aug-cc-pV(T+d)Z	–5.54	–2.17	+0.48	–0.40	+0.03	[–0.01]	[–7.61]
aug-cc-pV(Q+d)Z	–5.47	–2.13	+0.50	–0.40	[+0.03]	[–0.01]	[–7.48]
aug-cc-pV(5+d)Z	–5.43	–2.11	+0.52	–0.40	[+0.03]	[–0.01]	[–7.41]
CBS LIMIT	[–5.41]	[–2.09]	[+0.53]	[–0.40]	[+0.03]	[–0.01]	[–7.35]

E$_{int}$ =–7.35+1.97+0.08+0.02 = **–5.28**

anti-BrOH$\cdots$OH$_2$

	HF	+δ MP2	+δ CCSD	+δ (T)	+δ T	+δ (Q)	NET
aug-cc-pVDZ	–5.28	–2.17	+0.48	–0.43	+0.03	–0.01	–7.38
aug-cc-pVTZ	–5.09	–2.26	+0.49	–0.41	+0.03	[–0.01]	[–7.25]
aug-cc-pVQZ	–5.03	–2.24	+0.52	–0.41	[+0.03]	[–0.01]	[–7.14]
aug-cc-pV5Z	–4.99	–2.21	+0.52	–0.41	[+0.05]	[–0.01]	[–7.07]
CBS LIMIT	[–4.97]	[–2.18]	[+0.53]	[–0.41]	[+0.03]	[–0.01]	[–7.01]

E$_{int}$ = –7.01+1.95+0.07+0.02 = **–4.97**

The interaction energies for the halogen bonded dimers are much smaller than for the hydrogen bonded dimers (Table 2). The *anti*-HOCl$\cdots$OH$_2$ interaction energy is only –1.71 kcal mol^{-1}, which is 3.91 kcal mol^{-1} smaller than the strongest hydrogen bound dimer. Substituting the Cl atom with a bromine increases the magnitude of the interaction energy by 1.32 kcal mol^{-1} to –3.03 kcal mol^{-1}. Bromine is the only dimer with minima for both the *syn* and *anti* HOBr$\cdots$OH$_2$ structure. The *anti* isomer has a slightly larger interaction energy of –3.03 kcal mol^{-1} compared to –2.84 kcal mol^{-1} for the *syn* isomer. Halogen substi-

tution also has a significant impact on the ZPVE contribution, increasing it from 1.07 kcal mol^{-1} in the *anti*-HOCl-OH_2 structure to 1.21 kcal mol^{-1} in the *anti*-HOBr$\cdots OH_2$. The increase in the ZPVE is primarily do to a 100 cm^{-1} increase in the internal oxygen-halogen bond stretch mode of the HOX portion of the dimer. This trend is similar in magnitude but opposite in direction for the HB structures.

Table 2 Focal-point analysis fo the interaction energy of the halogen bonded HOX$\cdots OH_2$ structures in kcal mol^{-1}. The CCSD(T)/X2C-aug-cc-pVTZ equilibrium geometries were used for all computations here. Bracketed values indicate extrapolated energies or corrections. δ indicates an incremental change in energy from the previous level of theory. The CCSDT(Q)/X2C-CBS interaction energies and corrections are shown below in accordance to the formula: $E_{final} = E_{CCSDT(Q)-X2C/CBS} + \Delta E_{ZPVE} + \Delta E_{FC} + \Delta E_{DBOC}$

anti-HOCl$\cdots OH_2$

	HF	+δ MP2	+δ CCSD	+δ (T)	+δ T	+δ (Q)	NET
aug-cc-pV(D+d)Z	–1.17	–2.10	+0.52	–0.35	+0.02	–0.02	–3.10
aug-cc-pV(T+d)Z	–0.76	–2.35	+0.56	–0.38	+0.02	[–0.02]	[–2.92]
aug-cc-pV(Q+d)Z	–0.69	–2.36	+0.58	–0.39	[+0.02]	[–0.02]	[–2.86]
aug-cc-pV(5+d)Z	–0.68	–2.35	+0.59	–0.40	[+0.02]	[–0.02]	[–2.84]
CBS LIMIT	[–0.67]	[–2.34]	[+0.59]	[–0.40]	[+0.02]	[–0.02]	[–2.82]

E_{int} = –2.82+1.07+0.04+0.00= **–1.71**

anti-HOBr$\cdots OH_2$

	HF	+δ MP2	+δ CCSD	+δ (T)	+δ T	+δ (Q)	NET
aug-cc-pVDZ	–2.50	–2.67	+0.71	–0.41	+0.02	–0.02	–4.88
aug-cc-pVTZ	–1.82	–2.93	+0.75	–0.46	+0.03	[–0.02]	[–4.46]
aug-cc-pVQZ	–1.79	–2.90	+0.75	–0.48	[+0.03]	[–0.02]	[–4.42]
aug-cc-pV5Z	–1.78	–2.87	+0.75	–0.49	[+0.03]	[–0.02]	[–4.39]
CBS LIMIT	[–1.77]	[–2.84]	[+0.74]	[–0.49]	[+0.03]	[–0.02]	[–4.36]

E_{int} = –4.36+1.21+0.14-0.02 = **–3.03**

syn-HOBr$\cdots OH_2$

	HF	+δ MP2	+δ CCSD	+δ (T)	+δ T	+δ (Q)	NET
aug-cc-pVDZ	–2.27	–2.62	+0.69	–0.41	+0.02	–0.02	–4.60
aug-cc-pVTZ	–1.60	–2.88	+0.73	–0.46	+0.03	[–0.02]	[–4.20]
aug-cc-pVQZ	–1.57	–2.85	+0.73	–0.47	[+0.03]	[–0.02]	[–4.15]
aug-cc-pV5Z	–1.56	–2.81	+0.73	–0.48	[+0.03]	[–0.02]	[–4.12]
CBS LIMIT	[–1.55]	[–2.78]	[+0.72]	[–0.48]	[+0.03]	[–0.02]	[–4.08]

E_{int} =–4.08+1.10+0.14-0.00 = **–2.84**

Panek and Berski reported interaction energies for the same dimer structures at the MP2/aug-cc-pVTZ level of theory. For the XOH$\cdots OH_2$ dimers they report interaction energies of –7.45 kcal mol^{-1} for fluorine, –7.37 kcal mol^{-1} for chlorine, and –7.11 kcal mol^{-1} for bromine. These results are consistent with our quantitative trend for hydrogen bonds, but predict interaction energies of much greater magnitude than our focal point energies. Likewise, they also report interaction energies for the HOX$\cdots OH_2$ dimers of –2.68 kcal mol^{-1} for chlorine and –4.00 kcal mol^{-1} for bromine. Again, their interaction energies overestimate the magnitude of our focal point energies. Dibble and Francisco[27] report an interaction energy of –5.9 kcal mol^{-1} for *syn*-ClOH$\cdots OH_2$ at the MP4/6-311++G(3df,3pd)//MP2/6-311++G(d,p) level of theory. This energy is quite similar to our focal point energy of –5.56 kcal mol^{-1} but a bit larger in magnitude. For the bromine dimers, Santos and coworkers[76] report interaction energies of –4.1 kcal mol^{-1} for BrOH$\cdots OH_2$ at the CCSD/6-311++G(2d,2p) level of theory and –2.46 kcal mol^{-1} for HOBr$\cdots OH_2$ at the MP2/6-311++G(2d,2p)level of theory. The interaction energies from Santos are both lower in magnitude than the focal point predictions we present here.

Fig. 3 Primary natural bond orbital overlap interactions for the most favorable conformer of each dimer. The three hydrogen bonded structures appear first, followed by the halogen bonded structures. The black arrow signifies the donor acceptor relationship with the $E^{(2)}$ energy printed above in kcal mol^{-1}. The colors yellow, green, and purple represent F, Cl, and Br atoms, respectively.

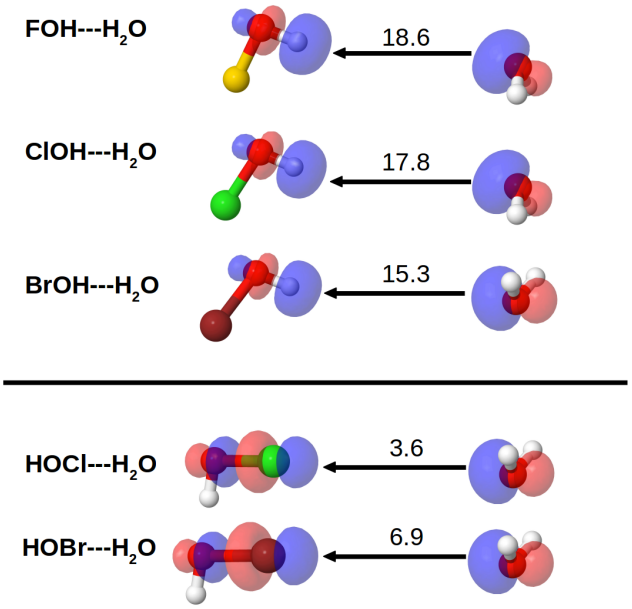

Natural Bond Orbital Analysis

NBO results are presented in Figure 3 and show the dominant orbital pair interactions. The primary interacting orbitals are similar for the *syn* and *anti* isomers in all structures; thus only the lowest energy isomer for each hydrogen and halogen bonded dimer are shown. For each dimer, the lone pair electrons from the oxygen of water donate into acceptor orbitals on the HOX monomer. The NBO scheme[102] produces an interaction energy (designated $E^{(2)}$ here) which is a ratio of the Fock matrix element between orbitals i and j and the difference between orbital energies ($\varepsilon_j - \varepsilon_i$). Thus a large $E^{(2)}$ energy corresponds to a large interaction between orbitals i and j. Figure 3 also presents the $E^{(2)}$ values between the donating and accepting orbitals. For the HB dimers, the interaction is dominated by the donation of the lone pair on the oxygen atom in water into a sigma bonding orbital in the HOX monomer. The energy of this interaction for the most favorable isomer is 18.6 kcal mol^{-1} for fluorine, 17.8 kcal mol^{-1} for chlorine, and 15.3 kcal mol^{-1} for bromine.

For the halogen bonded dimers, the primary orbital interaction is again the donation of the oxygen lone pair of water into a sigma bonding orbital of the HOX monomer, for which chlorine has a value of 3.75 kcal mol^{-1} and bromine 6.92 kcal mol^{-1}. This is consistent with the work of Oliveira and Kraka, which found for various halogen bonded systems that the primary NBO overlap is from the lone pair of an electron donor into the bonding orbital of the halogen atom and some electron withdrawing substituent at the CCSD(T)/aug-cc-pVTZ level of theory.[42] The increasing trend of the $E^{(2)}$ energy with increasing halogen size is the opposite of the trend observed with halogen bonded structures. Halogen

bonds are thought to form via the donation of electron density into a positive σ hole unoccupied orbital on the halogen[110], as seen in Figure 3. Based on our results, halogens of increasing size form larger σ holes that increase electron accepting ability. Halogen substitution has a much larger effect for the HOX$\cdots$OH$_2$ than the XOH$\cdots$OH$_2$ structures. For XB and HB dimers, respectively, the $\varepsilon_j - \varepsilon_i$ component of $E^{(2)}$ is essentially the same, and the Fock energy component is the primary contributor to changes in $E^{(2)}$, especially for the XB dimers.

Research by Zhang and coworkers[74] agrees qualitatively with our general trend that hydrogen bonds have greater $E^{(2)}$ energies than the the orbital overlap of halogen bonds. Zhang reports the primary orbital interaction energy for the ClOH$\cdots$OH$_2$ dimer's hydrogen-oxygen sigma bonding orbital overlap as 29.4 kcal mol^{-1}, compared to 10.3 kcal mol^{-1} for the oxygen-chlorine σ bond overlap of the HOCl$\cdots$OH$_2$ dimer for the same interaction. Other theoretical papers that studied other small organic compounds with hydrogen and halogen bonding saw a decrease in the $E^{(2)}$ energy for hydrogen bonds and an increase for halogen bonds when the halogen atom increases in size.[64,65,69,71,72]

SAPT Analysis

The interaction SAPT2+3 energy decomposition[108,111] for each dimer type is shown graphically in Figure 4. The lower energy *syn* conformers are shown for the HB dimers and the *anti* conformers for the XB dimers. All SAPT2+3 data is presented in detail in the supplementary information. For all nine dimers, the SAPT2+3 interaction energies, despite underestimating focal point interaction energies, were excellent qualitative estimates of the relative focal point interaction energies. However, the SAPT2+3 interaction energies were usually closer to the true interaction energies than a simpler scheme such as SAPT0 energies.[108,111] To determine the effect of geometry on the SAPT results, we ran our level of SAPT theory with the MP2 structures found by Panek and Berski.[73] The results from the MP2 structures and our CCSD(T) structures show differences of less than one kcal mol^{-1}.

It is helpful to examine the trends in the SAPT2+3 components across the periodic trends with increasing halogen size (Figure 4). The electrostatic component (labeled "elec") steadily decreases from fluorine to bromine in the HB structures. This correlates with the fact that the halogen atom increases in size and therefore has a more diffuse electron cloud. The same effect lowers the coulombic attraction between the donating lone pair and the acceptor. The trend is reversed for the XB dimers. Bromine forms a "more positive" σ hole than chlorine, increasing the electrostatic attraction from 4.8 kcal mol^{-1} to 8.1 kcal mol^{-1}.[37]

The exchange component (labeled "exch") is perhaps the most interesting, as it does not seem to follow a periodic trend for the XOH$\cdots$OH$_2$ dimers. The exchange energy increases from fluorine to chlorine but then decreases from chlorine to bromine. This might be due to the competition between atom size and spatial orientation with respect to the hydrogen bond. Increasing the size of the halogen atom will increase the orbital overlap of the halogen atom with the lone pair on the donating oxygen. This repulsion is alleviated by increasing the internal HOX bond angle as well as the HO$\cdots$X bond length, so much so that bromine is far enough away from the hydrogen bond that it does not contribute as much to the exchange component. In the halogen bond structures, the exchange is greatly dependent on the identity of the halogen. The exchange component nearly doubles from 6.5 kcal mol^{-1} for the chlorine structure to 10.7 kcal mol^{-1} when bromine is substituted.

Induction (ind) and dispersion (disp) contribute far less to the total SAPT2+3 interaction energies but are relevant because the exchange and electrostatic terms are opposite and nearly equal. This cancellation allows for induction and dispersion to impact the final interaction energies significantly.[36,112–114] For the HB dimers, induction decreases with substitution of larger halogen atoms. This is due to the decreasing electronegativities of larger halogens, which yield a smaller dipole. The opposite is true for the XB dimers where the σ hole on the halogen becomes more easily induced with a less electronegative atom like bromine. As expected, the dispersion term increases for all structures when the size of the halogen increases. It is important to note that in the HB dimers, changes in induction are larger than those for dispersion across the halogen series. For XB dimers, induction and dispersion work in tandem to increase the interaction energy.

Comparison of XB and HB

The structures presented in this study highlight the differences between hydrogen and halogen bonds, as modeled with high level *ab initio* theory. The most obvious result is the that the halogen bonds are generally weaker than the hydrogen bonds in all of our HOX-water dimers. Our results highlight two reasons why this is the case:

1. The halogen atoms are much larger compared to the hydrogen atom and therefore will form longer bonds. This larger distance greatly reduces the electrostatic attraction between atoms, which attraction is the primary driver for the bond formation based on the SAPT2+3 scheme[107].

2. The oxygen lone pair on water is better able to donate electron density to a hydrogen than a halogen atom on the HOX molecule. HOX compounds have a partial positive charge on their proton which easily accepts electron density from an oxygen lone pair. The dipole decreases with larger and less electronegative halogen atoms. The halogen bond is not caused because the halogen atom inherently has a partial positive charge, but because a positive sigma hole is induced on the halogen atom.[37,110] NBO supports this conclusion as $E^{(2)}$ increases as the size of the halogen increases. The larger halogens have greater polarizabilities which result in more positive sigma hole to accept the oxygen lone pair.

The dissociation energies of the XOH$\cdots$OH$_2$ dimers are much greater than those of the HOX$\cdots$OH$_2$ dimers, but close enough that both types of interactions may occur. The difference between our weakest halogen bond (HOCl$\cdots$OH$_2$= –1.71 kcal mol^{-1}) and our strongest hydrogen bond (FOH$\cdots$OH$_2$= –5.62 kcal mol^{-1})

Fig. 4 SAPT2+3/aug-cc-pVTZ decompositions are shown for the most energetically favorable conformer of each dimer. The decomposition is broken into favorable electrostatic (Elst), induction (Ind), and dispersion (Disp) terms, as well as unfavorable exchange (Exch) interaction.

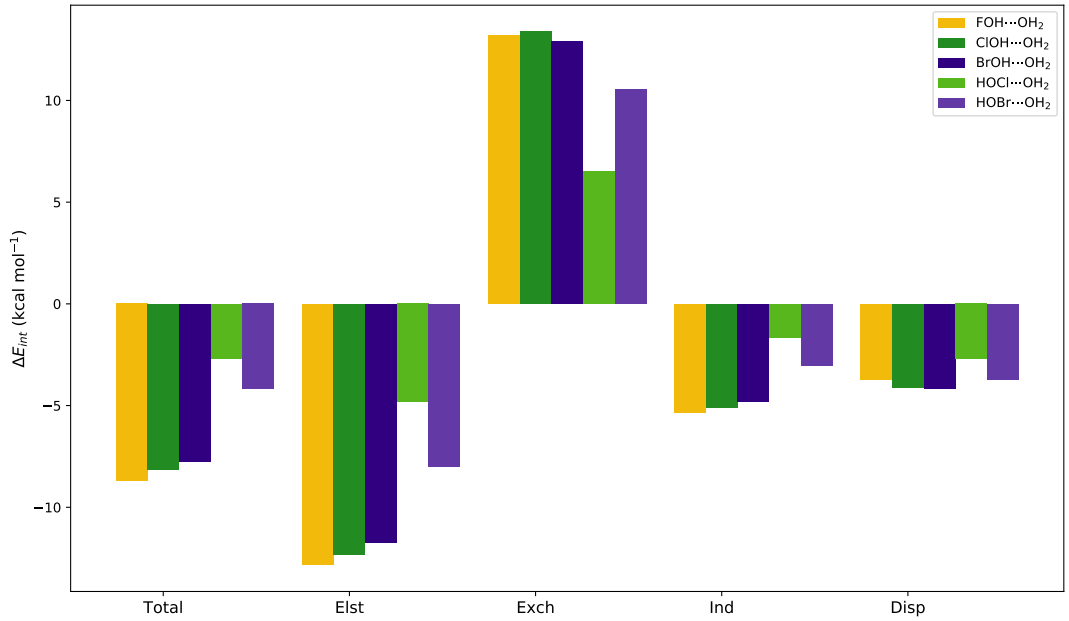

is 3.91 kcal mol^{-1}. Increasing halogen size lessens the gap between hydrogen and halogen bonds so much so that the difference between the focal point interaction energies of BrOH$\cdots$OH$_2$ (–4.97 kcal mol^{-1}) and HOBr$\cdots$OH$_2$ (–3.03 kcal mol^{-1}) is only 1.94 kcal mol^{-1}. This is relevant to atmospheric chemistry where HOBr molecules often bind to water.[1] Our results predicts that both hydrogen and halogen bonds may be present under atmospheric conditions. This may affect the mechanisms that lead to ozone depletion from HOX molecules.

Conclusions

Our work provides the most reliable theoretical study of hypohalous acid and water dimers to date. We have included extensive electron correlation with the CCSD(T) level of theory, used proper $+d$ basis sets for chlorine computations, and included relativistic effects with the SF-X2C-1e method. Our structures were found to have different geometric parameters than previous studies, most noteworthy being our shorter intermolecular bond lengths. Interaction energies were extrapolated to the complete basis set limit and CCSDT(Q) level of correlation. The interaction energies decrease in magnitude for the hydrogen bond dimers and increase for the halogen bond dimers when the size of the substituted halogen atom increases.

NBO and SAPT analyses were performed to compare the nature of each type of intermolecular interaction. NBO analysis displays the trends in electron donation from water to either the H or X of the HOX species. This donation decreases with increasing halogen size for HBs and increased for XBs. SAPT2+3 analysis showed that halogen substitution does impact both the interaction energies and the individual components, especially for halogen bound dimers. The largest change was due to the electrostatic interaction term.

Perhaps the most important result from this research is the large difference in interaction energies between a halogen bonded and hydrogen bonded dimer with the same atoms. For the chlorine and bromine dimers, the difference in interaction energies were around 4 kcal mol^{-1} and 2 kcal mol^{-1}, respectively. This confirms that even though hydrogen bonds are generally stronger than halogen bonds, they can become close enough in energy, with increasing halogen size that both interactions must be considered.[52–56] This may have consequences for atmospheric scientists studying the role of HOBr and HOCl in the depletion of ozone.

Conflicts of interest

There are no conflicts to declare.

Acknowledgements

This work was supported by U.S. National Science Foundation under grant number CHE-1661604.

Notes and references

1 J. P. D. Abbatt, *Geophys. Res. Lett.*, 1994, **21**, 665–668.
2 J. W. Adams, N. S. Holmes and J. N. Crowley, *Atmos. Chem. Phys.*, 2002, **2**, 79–91.
3 S. Solomon, R. R. Garcia, F. Sherwood Rowland and D. Wuebbles, *Nature*, 1986, **321**, 755–758.
4 Elliot, Scott, Cicerone, Ralph, Turco, Richard, Drdla, Katja and Tabazadeh, Azaddeh, *J. Geophys. Res.*, 1994.
5 R. Hossaini, M. P. Chipperfield, S. A. Montzka, A. Rap, S. Dhomse and W. Feng, *Nat. Geosci.*, 2015, **8**, 186–190.
6 K. A. Read, A. S. Mahajan, L. J. Carpenter, M. J. Evans,

B. V. E. Faria, D. E. Heard, J. R. Hopkins, J. D. Lee, S. J. Moller, A. C. Lewis, L. Mendes, J. B. McQuaid, H. Oetjen, A. Saiz-Lopez, M. J. Pilling and J. M. C. Plane, *Nature*, 2008, **453**, 1232–1235.

7 J. A. Schmidt, D. J. Jacob, H. M. Horowitz, L. Hu, T. Sherwen, M. J. Evans, Q. Liang, R. M. Suleiman, D. E. Oram, M. L. Breton, C. J. Percival, S. Wang, B. Dix and R. Volkamer, *J. Geophys. Res.-Atmos.*, 2016, **121**, 11,819–11,835.

8 T. Sherwen, J. A. Schmidt, M. J. Evans, L. J. Carpenter, K. Grobmann, S. D. Eastham, D. J. Jacob, B. Dix, T. K. Koenig, R. Sinreich, I. Ortega, R. Volkamer, A. Saiz-Lopez, C. Prados-Roman, A. S. Mahajan and C. Ordonez, *Atmos. Chem. Phys.*, 2016, **16**, 12239–12271.

9 T. K. Koenig, R. Volkamer, S. Baidar, B. Dix, S. Wang, D. C. Anderson, R. J. Salawitch, P. A. Wales, C. A. Cuevas, R. P. Fernandez, A. Saiz-Lopez, M. J. Evans, T. Sherwen, D. J. Jacob, J. Schmidt, D. Kinnison, J.-F. Lamarque, E. C. Apel, J. C. Bresch, T. Campos, F. M. Flocke, S. R. Hall, S. B. Honomichl, R. Hornbrook, J. B. Jensen, R. Lueb, D. D. Montzka, L. L. Pan, J. M. Reeves, S. M. Schauffler, K. Ullmann, A. J. Weinheimer, E. L. Atlas, V. Donets, M. A. Navarro, D. Riemer, N. J. Blake, D. Chen, L. G. Huey, D. J. Tanner, T. F. Hanisco and G. M. Wolfe, *Atmos. Chem. Phys.*, 2017, 1–46.

10 W. R. Simpson, U. Frieß, M. E. Goodsite, D. Heard, M. Hutterli, A. Richter, H. Roscoe, R. Sander, P. Shepson, J. Sodeau, A. Steffen, T. Wagner and E. Wolff, *Atmos. Chem. Phys.*, 2007, 44.

11 P. S. Monks, F. L. Nesbitt, M. Scanlon and L. J. Stief, *J. Phys. Chem.*, 1993, **97**, 11699–11705.

12 R. Müller, J.-U. Grooß, A. M. Zafar, S. Robrecht and R. Lehmann, *Atmos. Chem. Phys.*, 2018, **18**, 2985–2997.

13 W. A. Prütz, *Arch. Biochem. Biophys.*, 1999, **371**, 107–114.

14 M. Whiteman, A. Jenner and B. Halliwell, *Chem.Res.Toxicol.*, 1997, **10**, 1240–1246.

15 J. M. Albrich, C. A. McCarthy and J. K. Hurst, *Proc Natl Acad Sci U S A*, 1981, **78**, 210–214.

16 W. A. Prütz, R. Kissner, T. Nauser and W. H. Koppenol, *Arch. Biochem. Biophys.*, 2001, **389**, 110–122.

17 S. Sakarya, N. Gunay, B. Ozturk and B. Ertugrul, *Wounds*, 2014, **26**, 10.

18 G. Bhave, C. F. Cummings, R. M. Vanacore, C. Kumagai-Cresse, I. A. Ero-Tolliver, M. Rafi, J.-S. Kang, V. Pedchenko, L. I. Fessler, J. H. Fessler and B. G. Hudson, *Nat. Chem. Biol.*, 2012, **8**, 784–790.

19 E. L. Thomas, *Infect Immun*, 1979, **23**, 522–531.

20 C. L. Perrin and J. B. Nielson, *Annu. Rev. Phys. Chem.*, 1997, **48**, 511–544.

21 N. V. Belkova, E. S. Shubina and L. M. Epstein, *Acc. Chem. Res.*, 2005, **38**, 624–631.

22 G. R. Desiraju, *Acc. Chem. Res.*, 2002, **35**, 565–573.

23 K. Müller-Dethlefs and P. Hobza, *Chem. Rev.*, 2000, **100**, 143–168.

24 T. Kato and J. M. J. Frechet, *J. Am. Chem. Soc.*, 1989, **111**, 8533–8534.

25 A. M. S. Riel, D. A. Decato, J. Sun, C. J. Massena, M. J. Jessop and O. B. Berryman, *Chem. Sci.*, 2018, **9**, 5828–5836.

26 Y. Kim, K. H. Kim and C.-Y. Park, *B. Kor. Chem. Soc.*, 2005, **26**, 1953–1961.

27 T. S. Dibble and J. S. Francisco, *J. Phys. Chem.-US.*, 1995, **99**, 1919–1922.

28 M. Ortiz-Repiso, R. Escribano and P. C. Gómez, *J. Phys. Chem. A*, 2000, **104**, 600–609.

29 C. M. P. Santos, R. B. Faria, W. B. De Almeida, J. O. Machuca-Herrera and S. P. Machado, *Can. J. Chem.*, 2003, **81**, 961–970.

30 G. A. Jeffrey, *An introduction to hydrogen bonding*, Oxford University Press, New York, 1997.

31 S. Scheiner, *Hydrogen bonding: a theoretical perspective*, Oxford University Press, 1997.

32 A. D. Buckingham, J. E. Del Bene and S. A. C. McDowell, *Chem. Phys. Lett.*, 2008, **463**, 1–10.

33 K. B. Moore, K. Sadeghian, C. D. Sherrill, C. Ochsenfeld and H. F. Schaefer, *J. Chem. Theory Comput.*, 2017, **13**, 5379–5395.

34 A. Priimagi, G. Cavallo, P. Metrangolo and G. Resnati, *Acc. Chem. Res.*, 2013, **46**, 2686–2695.

35 A. C. Legon, *Phys. Chem. Chem. Phys.*, 2010, **12**, 7736–7747.

36 L. N. Anderson, F. W. Aquino, A. E. Raeber, X. Chen and B. M. Wong, *J. Chem. Theory Comput.*, 2018, **14**, 180–190.

37 G. Cavallo, P. Metrangolo, R. Milani, T. Pilati, A. Priimagi, G. Resnati and G. Terraneo, *Chem. Rev.*, 2016, **116**, 2478–2601.

38 M. G. Chudzinski and M. S. Taylor, *J. Org. Chem.*, 2012, **77**, 3483–3491.

39 M. H. Kolar and P. Hobza, *Chem. Rev.*, 2016, **116**, 5155–5187.

40 S. Kozuch and J. M. L. Martin, *J. Chem. Theory Comput.*, 2013, **9**, 1918–1931.

41 V. Oliveira, E. Kraka and D. Cremer, *Phys. Chem. Chem. Phys.*, 2016, **18**, 33031–33046.

42 V. Oliveira and E. Kraka, *J. Phys. Chem. A*, 2017, **121**, 9544–9556.

43 V. Oliveira, E. Kraka and D. Cremer, *Inorg. Chem.*, 2017, **56**, 488–502.

44 V. Oliveira and D. Cremer, *Chem. Phys. Let.*, 2017, **681**, 56–63.

45 J. Thirman, E. Engelage, S. M. Huber and M. Head-Gordon, *Phys. Chem. Chem. Phys.*, 2018, **20**, 905–915.

46 L. P. Wolters, P. Schyman, M. J. Pavan, W. L. Jorgensen, F. M. Bickelhaupt and S. Kozuch, *Wires. Comput. Mol. Sci.*, 2014, **4**, 523–540.

47 L. P. Wolters and F. M. Bickelhaupt, *ChemistryOpen*, 2012, **1**, 96–105.

48 A. Lange, J. Heidrich, M. O. Zimmermann, T. E. Exner and F. M. Boeckler, *J. Chem. Inf. Model.*, 2019.

49 V. Angarov and S. Kozuch, *New J. Chem.*, 2018, **42**, 1413–1422.

50 N. Galland, G. Montavon, J. L. Questel and J. Graton, *New*

J.Chem., 2018, **42**, 10510–10517.

51 Z. P. Shields, J. S. Murray and P. Politzer, *Int. J. Quantum Chem.*, 2010, **110**, 2823–2832.

52 Q.-Z. Li, B. Jing, R. Li, Z.-B. Liu, W.-Z. Li, F. Luan, J.-B. Cheng, B.-A. Gong and J.-Z. Sun, *Phys. Chem. Chem. Phys.*, 2011, **13**, 2266–2271.

53 Y. Geboes, F. De Proft and W. A. Herrebout, *Acta. Cryst. B*, 2017, **73**, 168–178.

54 S. W. L. Hogan and T. v. Mourik, *J. Comput. Chem.*, 2016, **37**, 763–770.

55 C. C. Robertson, J. S. Wright, E. J. Carrington, R. N. Perutz, C. A. Hunter and L. Brammer, *Chem. Sci.*, 2017, **8**, 5392–5398.

56 M. Domagala, A. Lutynska and M. Palusiak, *J. Phys. Chem. A*, 2018, **122**, 5484–5492.

57 K. V. Chance, D. G. Johnson and W. A. Traub, *J. Geophys. Res.*, 1989, **94**, 11059.

58 G. C. Toon and C. B. Farmer, *Geophys. Res. Lett.*, 1989, **16**, 1375–1377.

59 M. R. Le Breton, M. W. Gallagher, D. E. Shallcross, M. J. Evans, L. Carpenter, S. Andrews, R. T. Lidster, N. R. P. Harris and C. Percival, *AGU Fall Meeting Abstracts*, 2014, **23**, A23L–3434.

60 M. Dorf, A. Butz, C. Camy-Peyret, M. P. Chipperfield, L. Kritten and K. Pfeilsticker, *Atmos. Chem. Phys.*, 2008, 7.

61 E. H. Appelman, *Acc. Chem. Res.*, 1973, **6**, 113–117.

62 Q. Li, X. Xu, T. Liu, B. Jing, W. Li, J. Cheng, B. Gong and J. Sun, *Phys. Chem. Chem. Phys.*, 2010, **12**, 6837–6843.

63 X. An, H. Zhuo, Y. Wang and Q. Li, *J Mol Model*, 2013, **19**, 4529–4535.

64 A. Zabardasti, A. Sharifi-Rad and A. Kakanejadifard, *Spectrochim. Acta. A*, 2015, **151**, 746–759.

65 A. Zabardasti, Y. A. Tyula and H. Goudarziafshar, *J. Sulfur Chem.*, 2017, **38**, 119–133.

66 M. Solimannejad, I. Alkorta and J. Elguero, *Chem. Phys. Lett.*, 2007, **449**, 23–27.

67 A. Kakanejadifard, S. Japelaghi, M. Ghasemian and A. Zabardasti, *Struct. Chem.*, 2015, **26**, 23–33.

68 Q. Li, Q. Lin, W. Li, J. Cheng, B. Gong and J. Sun, *Chem. Phys. Chem.*, 2008, **9**, 2265–2269.

69 Q.-Z. Li, R. Li, P. Guo, H. Li, W.-Z. Li and J.-B. Cheng, *Comput. Theor. Chem.*, 2012, **980**, 56–61.

70 Q.-Z. Li, J.-L. Zhao, B. Jing, R. Li, W.-Z. Li and J.-B. Cheng, *J. Comput. Chem.*, **32**, 2432–2440.

71 A. Zabardasti, Y. A. Tyula and H. Goudarziafshar, *B. Chem. Soc. Ethiopia*, 2017, **31**, 241–252.

72 A. Zabaradsti, A. Kakanejadifard and M. Ghasemian, *Comput. Theor. Chem.*, 2012, **989**, 1–6.

73 J. J. Panek and S. Berski, *Chem. Phys. Lett.*, 2008, **467**, 41–45.

74 Z. Zhang, J. Shen, N. Jin, L. Chen and Z. Yang, *Comput. Theor. Chem.*, 2012, **999**, 48–54.

75 L. Ying and X. Zhao, *J. Phys. Chem. A*, 1997, **101**, 3569–3573.

76 C. M. P. Santos, R. Faria, S. P. Machado and W. B. De Almeida, *J. Chem. Phys.*, 2004, **121**, 141.

77 S. Qiao, L. Zhen, Z. Xiao Qing, G. Mao Fa and W. Dian Xu, *Chinese J. Chem.*, 2005, **23**, 483–490.

78 T. H. Dunning, K. A. Peterson and A. K. Wilson, *J. Chem. Phys.*, 2001, **114**, 9244–9253.

79 I. Shavitt and R. J. Bartlett, *Many-Body Methods in Chemistry and Physics: MBPT and Coupled-Cluster Theory*, Cambridge University Press, 2009.

80 J. F. Stanton, *Chem. Phys. Lett.*, 1997, **281**, 130–134.

81 R. J. Bartlett, J. D. Watts, S. A. Kucharski and J. Noga, *Chem. Phys. Lett.*, 1990, **165**, 513–522.

82 K. Raghavachari, G. W. Trucks, J. A. Pople and M. Head-Gordon, *Chem. Phys. Lett.*, 1989, **157**, 479–483.

83 M. E. Harding, T. Metzroth, J. Gauss and A. A. Auer, *J. Chem. Theory Comput.*, 2008, **4**, 64–74.

84 J. F. Stanton, J. Gauss, L. Cheng, M. E. Harding, D. A. Matthews and P. G. Szalay, *CFOUR, Coupled-Cluster techniques for Computational Chemistry, a quantum-chemical program package*, With contributions from A.A. Auer, R.J. Bartlett, U. Benedikt, C. Berger, D.E. Bernholdt, Y.J. Bomble, O. Christiansen, F. Engel, R. Faber, M. Heckert, O. Heun, M. Hilgenberg, C. Huber, T.-C. Jagau, D. Jonsson, J. Jusélius, T. Kirsch, K. Klein, W.J. Lauderdale, F. Lipparini, T. Metzroth, L.A. Mück, D.P. O'Neill, D.R. Price, E. Prochnow, C. Puzzarini, K. Ruud, F. Schiffmann, W. Schwalbach, C. Simmons, S. Stopkowicz, A. Tajti, J. Vázquez, F. Wang, J.D. Watts and the integral packages MOLECULE (J. Almlöf and P.R. Taylor), PROPS (P.R. Taylor), ABACUS (T. Helgaker, H.J. Aa. Jensen, P. Jørgensen, and J. Olsen), and ECP routines by A. V. Mitin and C. van Wüllen. For the current version, see http://www.cfour.de.

85 Q. Sun, W. Liu, Y. Xiao and L. Cheng, *J. Chem. Phys.*, 2009, **131**, 081101.

86 L. Cheng and J. Gauss, *J. Chem. Phys.*, 2011, **135**, 084114.

87 M. Iliaš and T. Saue, *J. Chem. Phys.*, 2007, **126**, 064102.

88 `http://slater.chemie.uni-mainz.de/cfour/index.php?n=Main.RecontractedCorrelation-consistentBasisFunctions`.

89 T. H. Dunning, *J. Chem. Phys.*, 1989, **90**, 1007–1023.

90 K. A. Peterson, C. Krause, H. Stoll, J. G. Hill and H.-J. Werner, *Molecular Physics*, 2011, **109**, 2607–2623.

91 M. K. Kesharwani, D. Manna, N. Sylvetsky and J. M. L. Martin, *J. Phys. Chem. A*, 2018, **122**, 2184–2197.

92 N. J. DeYonker, K. A. Peterson and A. K. Wilson, *J. Phys. Chem. A*, 2007, **111**, 11383–11393.

93 M. S. Schuurman, S. R. Muir, W. D. Allen and H. F. Schaefer, *J. Chem. Phys.*, 2004, **120**, 11586–11599.

94 J. M. Gonzales, C. Pak, R. S. Cox, W. D. Allen, H. F. Schaefer, A. G. Császár and G. Tarczay, *Chem.-Eur. J.*, 2003, **9**, 2173–2192.

95 A. G. Császár, W. D. Allen and H. F. Schaefer, *J. Chem. Phys.*, 1998, **108**, 9751–9764.

96 A. L. L. East and W. D. Allen, *J. Chem. Phys.*, 1993, **99**, 4638–

4650.

97 D. Feller, K. A. Peterson and T. D. Crawford, *J. Chem. Phys*, 2006, **124**, 054107.

98 T. Helgaker, W. Klopper, H. Koch and J. Noga, *J. Chem. Phys.*, 1997, **106**, 9639–9646.

99 N. C. Handy, Y. Yamaguchi and H. F. Schaefer, *J. Chem. Phys.*, 1986, **84**, 4481.

100 H. Sellers and P. Pulay, *Chem. Phys. Lett.*, 1984, **103**, 463–465.

101 D. E. Woon and T. H. Dunning, *J. Chem. Phys.*, 1995, **103**, 4572–4585.

102 E. D. Glendening, C. R. Landis and F. Weinhold, *Wires. Comput. Mol. Sci.*, 2012, **2**, 1–42.

103 E. D. Glendening, C. R. Landis and F. Weinhold, *J. Comput. Chem.*, 2013, **34**, 1429–1437.

104 Y. Shao, Z. Gan, E. Epifanovsky, A. T. B. Gilbert, M. Wormit, J. Kussmann, A. W. Lange, A. Behn, J. Deng, X. Feng, D. Ghosh, M. Goldey, P. R. Horn, L. D. Jacobson, I. Kaliman, R. Z. Khaliullin, T. Kús, A. Landau, J. Liu, E. I. Proynov, Y. M. Rhee, R. M. Richard, M. A. Rohrdanz, R. P. Steele, E. J. Sundstrom, H. L. Woodcock, P. M. Zimmerman, D. Zuev, B. Albrecht, E. Alguire, B. Austin, G. J. O. Beran, Y. A. Bernard, E. Berquist, K. Brandhorst, K. B. Bravaya, S. T. Brown, D. Casanova, C.-M. Chang, Y. Chen, S. H. Chien, K. D. Closser, D. L. Crittenden, M. Diedenhofen, R. A. DiStasio Jr., H. Dop, A. D. Dutoi, R. G. Edgar, S. Fatehi, L. Fusti-Molnar, A. Ghysels, A. Golubeva-Zadorozhnaya, J. Gomes, M. W. D. Hanson-Heine, P. H. P. Harbach, A. W. Hauser, E. G. Hohenstein, Z. C. Holden, T.-C. Jagau, H. Ji, B. Kaduk, K. Khistyaev, J. Kim, J. Kim, R. A. King, P. Klunzinger, D. Kosenkov, T. Kowalczyk, C. M. Krauter, K. U. Lao, A. Laurent, K. V. Lawler, S. V. Levchenko, C. Y. Lin, F. Liu, E. Livshits, R. C. Lochan, A. Luenser, P. Manohar, S. F. Manzer, S.-P. Mao, N. Mardirossian, A. V. Marenich, S. A. Maurer, N. J. Mayhall, C. M. Oana, R. Olivares-Amaya, D. P. O'Neill, J. A. Parkhill, T. M. Perrine, R. Peverati, P. A. Pieniazek, A. Prociuk, D. R. Rehn, E. Rosta, N. J. Russ, N. Sergueev, S. M. Sharada, S. Sharmaa, D. W. Small, A. Sodt, T. Stein, D. Stück, Y.-C. Su, A. J. W. Thom, T. Tsuchimochi, L. Vogt, O. Vydrov, T. Wang, M. A. Watson, J. Wenzel, A. White, C. F. Williams, V. Vanovschi, S. Yeganeh, S. R. Yost, Z.-Q. You, I. Y. Zhang, X. Zhang, Y. Zhou, B. R. Brooks, G. K. L. Chan, D. M. Chipman, C. J. Cramer, W. A. Goddard, M. S. Gordon, W. J. Hehre, A. Klamt, H. F. Schaefer, M. W. Schmidt, C. D. Sherrill, D. G. Truhlar, A. Warshel, X. Xua, A. Aspuru-Guzik, R. Baer, A. T. Bell, N. A. Besley, J.-D. Chai, A. Dreuw, B. D. Dunietz, T. R. Furlani, S. R. Gwaltney, C.-P. Hsu, Y. Jung, J. Kong, D. S. Lambrecht, W. Liang, C. Ochsenfeld, V. A. Rassolov, L. V. Slipchenko, J. E. Subotnik, T. Van Voorhis, J. M. Herbert, A. I. Krylov, P. M. W. Gill and M. Head-Gordon, *Mol. Phys.*, 2015, **113**, 184–215.

105 C. Lee, W. Yang and R. G. Parr, *Phys. Rev. B*, 1988, **37**, 785–789.

106 E. Willighagen, E. Willighagen and M. Howard, *Nature Precedings*, 2007.

107 E. G. Hohenstein and C. D. Sherrill, *J Chem Phys*, 2010, **133**, 014101.

108 B. Jeziorski, R. Moszynski and K. Szalewicz, *Chem. Rev.*, 1994, **94**, 1887–1930.

109 R. M. Parrish, L. A. Burns, D. G. A. Smith, A. C. Simmonett, A. E. DePrince, E. G. Hohenstein, U. Bozkaya, A. Y. Sokolov, R. Di Remigio, R. M. Richard, J. F. Gonthier, A. M. James, H. R. McAlexander, A. Kumar, M. Saitow, X. Wang, B. P. Pritchard, P. Verma, H. F. Schaefer, K. Patkowski, R. A. King, E. F. Valeev, F. A. Evangelista, J. M. Turney, T. D. Crawford and C. D. Sherrill, *J. Chem. Theory Comput.*, 2017, **13**, 3185–3197.

110 P. Politzer, J. S. Murray and M. C. Concha, *J. Mol. Model.*, 2007, **13**, 643–650.

111 E. G. Hohenstein and C. D. Sherrill, *Wires. Comput. Mol. Sci.*, 2012, **2**, 304–326.

112 K. E.Riley and P. Hobza, *Phys. Chem. Chem. Phys.*, 2013, **15**, 17742–17751.

113 K. E. Riley, J. S. Murray, J. Fanfrlik, J. Rezac, R. J. Sola, M. C. Concha, F. M. Ramos and P. Politzer, *J. Mol. Model*, 2013, **19**, 4651–4659.

114 P. Politzer, K. E. Riley, F. A. Bulat and J. S. Murray, *Comput.Theor. Chem.*, 2012, **998**, 2–8.

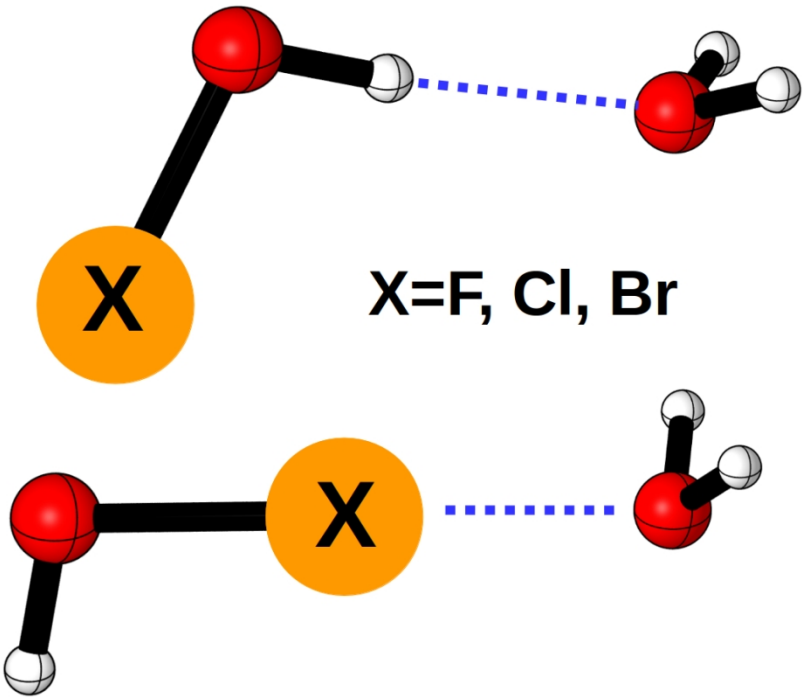

467x366mm (72 x 72 DPI)